

Tunneling effects and intersubband absorption in AlN/GaN superlattices

E. Baumann, F. R. Giorgetta,^{a)} and D. Hofstetter
 University of Neuchâtel, 1 A.-L. Breguet, Neuchâtel, CH 2000, Switzerland

H. Wu, W. J. Schaff, and L. F. Eastman
 415 Phillips Hall, Cornell University, Ithaca, New York 14850

L. Kirste
 Fraunhofer-Institute of Applied Solid State Physics, Tullastrasse 72, Freiburg, D-79108, Germany

We report on intersubband absorption and photovoltage measurements on regular GaN/AlN-based superlattice structures. For barrier thicknesses larger than about 25 Å, the optical intersubband absorption peaks at a considerably smaller energy than the photovoltage spectrum. A simple model taking into account the oscillator strength of the involved transitions and the corresponding tunneling probabilities agrees with the experimental findings. According to this model, the observed photovoltage is the macroscopic manifestation that the two-dimensional electron gas at the top of the superlattice changes its carrier density by a vertical transport of electrons.

Thanks to their large band gap energies, the semiconductor materials GaN and AlN have attracted a lot of attention for the fabrication of long-lived visible lasers and light-emitting diodes.¹⁻³ More recently, the huge conduction band discontinuity of nearly 2 eV between these two semiconductors has resulted in some device proposals based on intersubband transitions.⁴⁻⁶ Particularly interesting in this context are photodetectors, modulators, or lasers in the technologically interesting 1.55 μm wavelength range. Such devices could profit from short intersubband lifetimes, which might eventually result in high operating frequencies.^{7,8} Unfortunately, the heavy effective masses of 0.2 m_e for GaN and 0.32 m_e for AlN impose the epitaxial growth of layer thicknesses in the 15–30 Å range, which, despite substantial progress in molecular beam epitaxy, is still quite a challenging task.⁹ Nevertheless, intersubband absorption down to 1.06 μm has been shown in heavily doped, ultrathin GaN quantum wells which were separated by barriers of either AlGaIn, pure AlN, or AlN/GaN superlattices.^{10,11} In the majority of these experiments, the observed effects were purely optical and, except for one report, no vertical current transport could be demonstrated.¹² In a different type of experiment, one research group reported transport through thin AlN barriers in a resonant tunneling diode.¹³ In our present work, we see the combined effects of intersubband absorption and tunneling in a regular AlN/GaN superlattice.

All our measurements have been carried out on epitaxial material grown by molecular beam epitaxy on C-face sapphire substrates.¹⁴ Growth started with a 500-nm-thick *n*-type AlGaIn buffer layer (Si, $5 \times 10^{19} \text{ cm}^{-3}$) with a high Al content, typically between 67% and 100%. Exact numbers have been measured using high-resolution x-ray diffraction and are shown in Table I. The active region consists of a regular 20 period superlattice with undoped AlN barriers and degenerately doped GaN quantum wells (Si, $5-10 \times 10^{19} \text{ cm}^{-3}$) and is typically about 50% relaxed. The well thicknesses range from 17 to 38 Å, while the barriers are between 18 and 34 Å thick. Finally, the multiple quantum

well structure of all samples was covered with a 100 nm AlGaIn cap layer of the same composition and doping as the buffer. This cap layer is partly relaxed. Lateral resistance measurements in the AlGaIn buffer have shown that even such a high doping level does not lead to appreciable conductivity, especially if the Al content exceeds 80%.¹⁵ Sample preparation for optical absorption measurements relied on polishing of 3-mm-long and 300-μm-thick multipass waveguides as shown schematically in the inset of Fig. 1. The polishing process was followed by electrical contact evaporation. The contact stripes were ohmic (Ti/Al, 40/400 nm, annealed at 800 °C for 60 s), covered the entire sample length, had a width of 800 μm, and were separated by 1200 μm (edge to edge).

For the photovoltage measurements, the copper platelets holding the sample were mounted on the cold finger of a liquid He-flow cryostat held at a constant temperature of 10 K. In contrast, all optical absorption measurements were done at 300 K. The cryostat was placed into the sample compartment of a Fourier transform infrared spectrometer. For absorption measurements, the sample was used in transmission geometry; and the transmitted signal was measured with a liquid nitrogen cooled mercury–cadmium–telluride detector. During the photovoltaic measurements, the sample itself served as a detector. In both cases, illumination was accomplished by the spectrometer’s internal white light source.

TABLE I. Structural properties of the nitride samples used for these experiments. Data were obtained from x-ray diffraction. The doping density indicated stands for the wells in the superlattice structure.

Sample	Al content	Well/barrier thickness (Å)	Nominal/measured doping (cm^{-3})
A	98%	38/19	$0.8/1.2 \times 10^{20}$
B	67%	33/34	$1.0/0.6 \times 10^{20}$
C	90%	22/23	$0.5/1.2 \times 10^{20}$
D	100%	17/18	$1.0/0.5 \times 10^{20}$

^{a)}Electronic mail: fabrizio.giorgetta@unine.ch

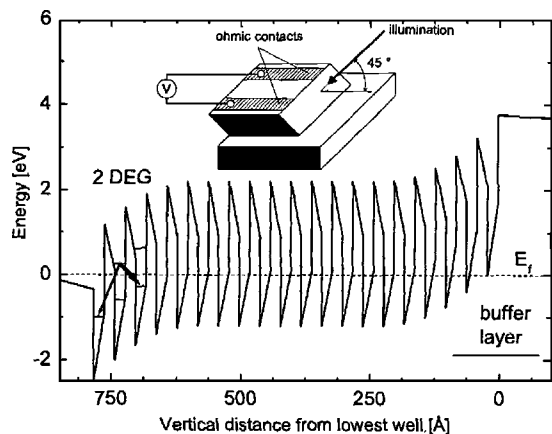


FIG. 1. Schematic conduction band diagram of our multiple quantum well structures. Illumination excites electrons into the upper bound state of the wells from where they drop into an adjacent well. The field gradient in the 2DEG region dictates that a net electron transport toward the sample surface is established. The inset shows the geometry of the sample on the copper platelet.

Due to spontaneous and strain-induced polarization effects, a two-dimensional electron gas (2DEG) is formed at the superlattice/cap layer interface; whereas a two-dimensional hole gas builds up at the superlattice/buffer layer interface.¹⁶ Voltage versus current curves confirmed that the annealed top contact goes all the way through the cap and makes contact to the 2DEG. Under illumination, electrons are lifted into the excited states of the wells from where they drop either back or into an adjacent well. For the latter case, the field gradient in the 2DEG region promotes tunneling toward the cap and hampers tunneling in the direction of the buffer. Therefore, although not being very efficient, a net electron transport towards the AlGaIn cap is established, the 2DEG is slightly enhanced, and a negative voltage occurs at the illuminated top contact. At the dark contact, however, no enhancement will take place and no voltage builds up. By measuring between an illuminated and a dark contact, we are thus able to see a photovoltaic signal whose sign depends on the position of the light spot on the sample.

Figure 2 presents optical intersubband absorption and photovoltage measurements for all samples. All absorption curves were obtained by dividing the p -polarized sample transmission spectrum by the p -polarized spectrum of the internal white light source, followed by the normalization

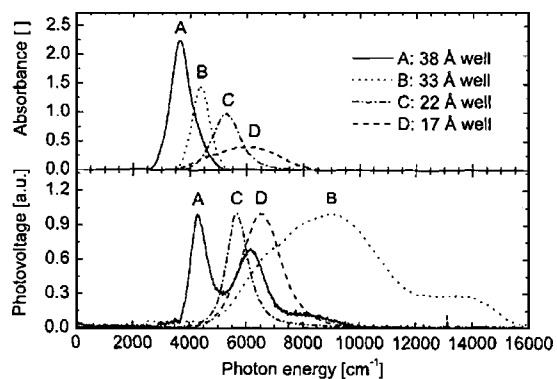


FIG. 2. Comparison of optical intersubband absorption and photovoltage spectra. The photovoltage in p polarization was normalized to 1 whereas the optical absorption is shown in absorbance units.

$\alpha(\nu) \times L = -\ln(I_{\text{sample}}/I_{\text{white}})$ with $L=3$ mm. With decreasing well width, a transition energy increase due to quantum confinement is clearly visible. According to Fermi's golden rule, the surface under the absorption curves is proportional to the oscillator strength of the optical transition. Nominal and computed doping densities are shown in Table I and agree reasonably well. From the amount of linewidth broadening, one can deduce an approximate number for the interfacial roughness of the layers. A naive comparison of samples A and B, and of samples C and D, which each have 5 Å well width difference, i.e., about one monolayer on each side, reveals that the thickness fluctuation in all wells must be on the order of roughly one monolayer (2.4 Å). This becomes clear once we notice that curve A drops to about half of its maximum value at the photon energy where curve B is maximal, and vice versa. Especially for samples C and D, s -polarized absorption and photovoltage peaks were not negligibly small. This apparent violation of the polarization selection rule is a result of polarization coupling, interface roughness, and the standing wave effect in the active layer. As far as vertical transport goes, samples C and D show the expected behavior: Absorption takes place at the lower edge of the miniband formed by the coupled first excited states while due to an enhanced tunneling probability, vertical transport is more probable to happen at the upper edge.

In contrast to samples C and D, samples A and B reveal a significant difference between the absorption and the transport spectra. In sample A, the fundamental absorption peak still shows up in the photovoltage spectrum, although accompanied by at least two other transitions. In sample B, however, the photovoltage peaks at a completely different energy than the absorption. In addition, its relative full width at half maximum is so much larger than in the other samples, that we strongly believe that multiple transitions into higher energetic states are at the origin of this broad signal. The reasons for this rather peculiar behavior can be understood on the basis of the following model. In first approximation, the photovoltage for each transition is a Gaussian whose height is proportional to the corresponding oscillator strength times a tunneling probability computed via the Wentzel-Kramers-Brillouin method times the blackbody spectral intensity of the illumination source.¹⁷ Since both barrier height and thickness are different for different transitions, the respective tunneling probabilities can vary by many orders of magnitude. It is therefore possible that a transition into a higher excited state, although having a very small oscillator strength, becomes the dominant one for transport. This is exactly what happened for samples A and B: they have thick wells (A: 38 Å, B: 33 Å) which contain the two lowest confined states in the triangular section of the well. In addition, sample B has an extremely thick barrier of 34 Å, which makes tunneling from the first excited state into a neighboring well's ground state very unlikely.

In order to further understand the functioning of our samples, we investigated the transient behavior of sample D at different temperatures. The left half of Fig. 3 shows such a series of photovoltaic measurements as a function of time and between 5 and 180 K. Time was measured from the onset of the illumination with the spectrometer's internal white light source (25 mW total power). After each measurement, the temperature was ramped up to 313 K in order to maintain identical starting conditions. At temperatures below 80 K, the photovoltage jumps abruptly to about half of its

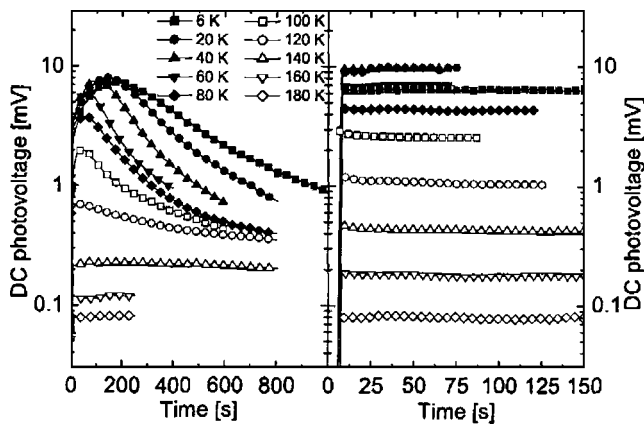


FIG. 3. Left panel: transient behavior of the dc component of the photovoltaic signal under strong illumination with a halogen lamp. Right panel: the same measurements with a silicon wafer used as optical filter.

maximum value, increases more slowly up to the maximum, and finally decreases toward zero. The signal changes after the sharp initial increase are faster at higher temperatures. All these observations are consistent with the simultaneous occurrence of an intersubband absorption/tunneling process, persistent photoconductivity, and optical quenching of photoconductivity in the GaN wells. Hence, if one of the two identical ohmic contacts is illuminated, the 2DEG at the superlattice/cap layer interface will be quickly enhanced by the intersubband mechanism described in Fig. 1; this lifts the Fermi energy and results instantly in a negative voltage at this contact.¹⁸ This voltage becomes larger if the lateral conductivity in the wells is low and vice versa; and the latter is strongly influenced by parasitic effects due to midgap states. Since the spectrometer's white light source is filtered only by the ZnSe window of the cryostat, photon energies up to 2.5 eV are available. As Ursaki,¹⁹ Hirsch,²⁰ and McCluskey²¹ have pointed out, this is sufficiently large to release trapped electrons and holes from their midgap states into the conduction and the valence band, respectively. In addition, it has been observed by other groups that optical quenching takes place on a different, faster time scale than the persistent photoconductivity.¹⁹ For this reason, we initially see a signal increase (conductivity decrease) which lasts up to 200 s; afterwards the signal decays more slowly toward zero (conductivity increase). In agreement with earlier publications about photoconductivity, the concomitant signal decay is much slower at low temperatures than at 180 K. Below 80 K, the measured signal dropped even below zero; but this could be an artifact due to an insufficiently long recovery heating at 313 K. In Fig. 3 (left panel), we corrected for this effect by adding a small constant of 1 mV to the curves of 5, 20, 40, 60, and 80 K. In order to suppress the photoinduced carrier release, we re-measured the curves from Fig. 3 (left panel) using a silicon wafer as an optical filter (absorbing for $\lambda < 1.1 \mu\text{m}$). During these measurements, the optical threshold for electron/hole release was not reached and thus no signal decay was observed (see Fig. 3, right panel).

In conclusion, we have presented results which show unambiguously the signature of vertical transport in AlN/

GaN-based superlattices. The main argument is based on the fact that optical absorption can peak at completely different wavelengths than the photovoltaic measurements. Especially if the barriers were very thick and high, we observed higher order transitions, whereas the first excited state did not dominate the spectrum or not even show up. Temperature-dependent measurements on one sample revealed furthermore the detrimental effects of persistent photoconductivity in GaN.

The authors thank the Professorship Program and the National Center of Competence in Research "Quantum Photonics" both of the Swiss National Science Foundation, the US Office of Naval Research under the NICOP and the MURI programs, as well as the European Project NITWAVE (contract 004170) for their generous financial support. Helpful discussions with Lubos Hvozdar (Alpes Lasers, SA, Neuchatel, Switzerland) and technical assistance from Julien Dorsaz (EPFL, Lausanne, Switzerland) and Xavier Niquille (Institute of Microtechnology, University of Neuchatel, Switzerland) are also gratefully acknowledged.

- ¹S. Nagahama, T. Yanamoto, M. Sano, and T. Mukai, *Appl. Phys. Lett.* **79**, 1948 (2001).
- ²M. Kneissl, D. W. Treat, M. Teepe, N. Miyashita, and N. M. Johnson, *Appl. Phys. Lett.* **82**, 4441 (2003).
- ³S. Nakamura, M. Senoh, N. Iwasa, and S. I. Nagahama, *Appl. Phys. Lett.* **67**, 1868 (1995).
- ⁴O. Ambacher, J. Majewski, C. Miskys, A. Link, M. Hermann, M. Eickhoff, M. Stutzmann, F. Bernardini, V. Fiorentini, V. Tilak, B. Schaff, and L. F. Eastman, *J. Phys.: Condens. Matter* **14**, 3399 (2002).
- ⁵C. Gmachl, H. M. Ng, and A. Y. Cho, *Appl. Phys. Lett.* **79**, 1590 (2001).
- ⁶T. Vurgaftman and J. R. Meyer, *J. Appl. Phys.* **94**, 3675 (2003).
- ⁷J. D. Heber, C. Gmachl, H. M. Ng, and A. Y. Cho, *Appl. Phys. Lett.* **81**, 1237 (2002).
- ⁸N. Iizuka, K. Kaneko, N. Suzuki, T. Asano, S. Noda, and O. Wada, *Appl. Phys. Lett.* **77**, 648 (2000).
- ⁹A. Helman, M. Tchernycheva, A. Lusson, E. Warde, F. H. Julien, K. Mounanis, G. Fishman, E. Monroy, B. Daudin, D. L. Dang, E. Bellet-Amalric, and D. Jalabert, *Appl. Phys. Lett.* **83**, 5196 (2003).
- ¹⁰C. Gmachl, H. M. Ng, S. G. Chu, and A. Y. Cho, *Appl. Phys. Lett.* **77**, 3722 (2000).
- ¹¹A. Kikuchi, H. Kanazawa, and T. Tachibana, *Appl. Phys. Lett.* **81**, 1234 (2002).
- ¹²D. Hofstetter, S.-S. Schad, H. Wu, W. J. Schaff, and L. F. Eastman, *Appl. Phys. Lett.* **83**, 572 (2003).
- ¹³A. Kikuchi, R. Bannai, K. Kishino, C. M. Lee, and J. I. Chyi, *Appl. Phys. Lett.* **81**, 1729 (2002).
- ¹⁴M. J. Murphy, K. Chu, H. Wu, W. Yeo, W. J. Schaff, O. Ambacher, J. Smart, J. R. Shealy, and L. F. Eastman, *J. Vac. Sci. Technol. B* **17**, 1252 (1999).
- ¹⁵D. Korakakis, H. M. Ng, K. F. Ludwig, Jr, and T. D. Moustakas, *Mater. Res. Soc. Symp. Proc.* **449**, 233 (1997).
- ¹⁶R. Dimitrov, M. Murphy, J. Smart, W. J. Schaff, J. R. Shealy, L. F. Eastman, O. Ambacher, and M. Stutzmann, *J. Appl. Phys.* **87**, 3375 (2000).
- ¹⁷F. Capasso, K. Mohammed, and A. Y. Cho, *IEEE J. Quantum Electron.* **22**, 1853 (1986).
- ¹⁸J. A. Smart, A. T. Schremer, N. G. Weimann, O. Ambacher, L. F. Eastman, and J. R. Shealy, *Appl. Phys. Lett.* **75**, 388 (1999).
- ¹⁹V. V. Ursaki, I. M. Tiginyanu, P. C. Ricci, A. Anedda, S. Hubbard, and D. Pavlidis, *J. Appl. Phys.* **94**, 3875 (2003).
- ²⁰M. T. Hirsch, J. A. Wolk, W. Walukiewicz, and E. E. Haller, *Appl. Phys. Lett.* **71**, 1098 (1997).
- ²¹M. D. McCluskey, N. M. Johnson, C. G. Walle, D. P. Bour, M. Kneissl, and W. Walukiewicz, *Phys. Rev. Lett.* **80**, 4008 (1998).